

PAPER • OPEN ACCESS

Numerical study on slip effects on aligned magnetic field flow over a permeable stretching surface with thermal radiation and viscous dissipation

To cite this article: Seethi Reddy Reddisekhar Reddy *et al* 2017 *IOP Conf. Ser.: Mater. Sci. Eng.* **263** 062003

View the [article online](#) for updates and enhancements.

Related content

- [Principles of Biophotonics, Volume 2: Black body radiation](#)
G Popescu
- [Effect of viscous dissipation of a magneto hydrodynamic micropolar fluid with momentum and temperature dependent slip flow](#)
K Gangadhar, Sathies Kumar, K Lakshmi Narayana et al.
- [The stagnation-point flow and heat transfer of nanofluid over a shrinking surface in magnetic field and thermal radiation with slip effects : a stability analysis](#)
N S Ismail, N M Arifin, R Nazar et al.

Numerical study on slip effects on aligned magnetic field flow over a permeable stretching surface with thermal radiation and viscous dissipation

Seethi Reddy Reddisekhar Reddy, P Bala Anki Reddy and N Sandeep

Department of Mathematics, School of Advanced Sciences, VIT University, Vellore-632014, India

E-mail: bala.anki@vit.ac.in

Abstract. This work concentrates on the study of the unsteady hydromagnetic heat and mass transfer of a Newtonian fluid in a permeable stretching surface with viscous dissipation and chemical reaction. Thermal radiation, velocity slip, concentration slip are also considered. The unsteady in the flow, velocity, temperature and concentration distribution is past by the time dependence of stretching velocity surface temperature and surface concentration. Appropriate similarity transformations are used to convert the governing partial differential equations into a system of coupled non-linear differential equations. The resulting coupled non-linear differential equations are solved numerically by using the fourth order Runge-Kutta method along with shooting technique. The impact of various pertinent parameters on velocity, temperature, concentration, skin friction coefficient, Nusselt number and the Sherwood number are presented graphically and in tabular form. Our computations disclose that fluid temperature has inverse relationship with the radiation parameter.

1. Introduction

The concept of boundary layer flow of heat and mass transfer of stretching surfaces has gained the interest of many researchers because of its have more engineering applications and also industrial manufacturing processes. Some examples are in the glass blowing, crystal growing, nuclear reactors, cooling of metallic sheets or electronic chips, extraction rubber sheets, wire drawing, hot rolling, the spinning of fibers, metal spinning, paper production, manufacture of foods, etc. Mastroberardino [1] found accurate solutions for viscoelastic flow over a stretching sheet. In addition, we have treated two types of chemical reactions one is homogeneous (involving within a single phase) and another one is heterogeneous (involving two or more phases). It depends on whether they occur at an interface or as a homogeneous reaction. (Byron Bird R. et al. [2]) During a chemical reaction heat is generated between two species. Some authors [3-7] investigated the steady two-dimensional Magnetohydrodynamic flow of a stretching sheet/surface with thermal radiation and chemical reaction. Suneetha and Bala Anki Reddy [8] carried out to describe the heat and mass transfer of viscous fluid over the stretching cylinder with chemical reaction.

Radiation effect in blood flow has got significant applications in physics (nuclear plants, space satellites, aircraft and gas turbines) and biomedical engineering medical treatment methods (myalgia, muscle spasms and chronic wide-spread pain). Sharidan [9] examined the unsteady boundary layer flow



over a stretching sheet. Several studies on the heat source/sink and thermal radiation effects were completed by some researchers [10-18].

The intent of the current model is the study of the unsteady hydromagnetic heat and mass transfer of a Newtonian fluid in a permeable stretching surface with viscous dissipation and chemical reaction. viscous dissipation, velocity slip, thermal slip and solutal slip conditions are taken into account.

2. Mathematical formulation

Let us consider an unsteady flow of the heat and mass transfer of a Newtonian fluid in a permeable stretching sheet. At time $t=0$, the sheet is stretched with velocity $U_w(x,t) = ax/(1-ct)$ along the x -axis. The aligned magnetic field $B(t)$ is applied perpendicular to the sheet. It is assumed that the magnetic Reynolds number is much less than unity. The governing boundary layer equations are

$$\frac{\partial u}{\partial x} + \frac{\partial v}{\partial y} = 0 \quad (1)$$

$$u \frac{\partial u}{\partial x} + v \frac{\partial u}{\partial y} + \frac{\partial u}{\partial t} = \nu \frac{\partial^2 u}{\partial y^2} + g\beta^*(C - C_\infty) + g\beta(T - T_\infty) - \frac{\sigma B^2(t)}{\rho} \sin^2(\xi)u - \frac{\nu}{k_1(t)}u \quad (2)$$

$$u \frac{\partial T}{\partial x} + v \frac{\partial T}{\partial y} + \frac{\partial T}{\partial t} = \frac{k}{\rho C_p} \frac{\partial^2 T}{\partial y^2} - \frac{1}{\rho C_p} \frac{\partial q_r}{\partial y} + \frac{q'''}{\rho C_p} + \frac{\nu}{C_p} \left(\frac{\partial u}{\partial y} \right)^2 \quad (3)$$

$$u \frac{\partial C}{\partial x} + v \frac{\partial C}{\partial y} + \frac{\partial C}{\partial t} = D \frac{\partial^2 C}{\partial y^2} - \Gamma(t)(C - C_\infty). \quad (4)$$

Let us consider $B(t) = B_0(1-ct)^{-\frac{1}{2}}$ and $\Gamma(t) = \Gamma_0(1-ct)^{-1}$, where B_0 , Γ_0 are the constants, u is the velocity component in the x and v is the velocity component in the y direction. β , β^* are the coefficient of thermal and concentration expansion respectively. ξ is the aligned angle, $k_1(t) = k_2(1-ct)$ is the time-dependent permeability parameter, D is the mass diffusion coefficient. Subject to the boundary conditions:

$$u - U_w = N\mu \frac{\partial u}{\partial y}, v = V_w, T - T_w = K \frac{\partial T}{\partial y}, C = C_w P \frac{\partial C}{\partial y} \text{ at } y=0$$

$$u \rightarrow 0, T \rightarrow T_\infty, C \rightarrow C_\infty \text{ as } y \rightarrow \infty \quad (5)$$

where V_w represents the injection/suction velocity given by

$$V_w = -\sqrt{\nu U_w / x} f(0) \quad (6)$$

Where V_w ($V_w > 0, V_w < 0$ are injection and suction respectively) represent the velocity of mass transfer at the surface of the capillary wall. In Eq. (5), $N = N_0(1-ct)^{1/2}$, $K = K_0(1-ct)^{1/2}$ and $P = P_0(1-ct)^{1/2}$ are the velocity slip, thermal slip and concentration slip factors respectively. $U_w(x,t), T_w(x,t)$ and $C_w(x,t)$ are the velocity, surface temperature and concentration, which are considered as

$$U_w = \frac{ax}{1-ct}, T_w = T_\infty + \frac{bx}{1-ct}, C_w = C_\infty + \frac{dx}{1-ct} \quad (7)$$

where a, b, c and d are the constants such that

$$a > 0, b \geq 0, c \geq 0, d \geq 0 \text{ and } ct < 1.$$

The non-uniform heat source/sink, q''' is modeled as, $q''' = \frac{KU_w(x,t)}{x\nu} [A^*(T_w - T_\infty)f' + (T - T_\infty)B^*]$

where A^* and B^* are the coefficient of space and temperature dependent heat source/sink,

respectively. If $A^* > 0, B^* > 0$ and $A^* < 0, B^* < 0$ heat generation and heat absorption respectively. The radiative heat flux q_r is given by

$$q_r = -\frac{4\sigma^*}{3k^*} \frac{\partial T^4}{\partial y}, \quad (8)$$

Where σ^*, k^* are the Stefan–Boltzmann constant and Rosseland mean absorption coefficient respectively. It should be noted that, the present analysis is limited to optically thick fluids. If the temperature differences within the mass of blood flow are sufficiently small, then Eq. (8) can be linearized by expanding T^4 into Taylor's series about T_∞ , and neglecting higher-order terms, we get,

$$T^4 \cong 4T_\infty^3 T - 3T_\infty^4 \quad (9)$$

We introduce the self-similar transformations

$$\eta = \left(\frac{U_w}{\nu x}\right)^{\frac{1}{2}} y, \quad \psi = (\nu x U_w)^{\frac{1}{2}} f(\eta), \quad \theta(\eta) = \frac{T - T_\infty}{T_w - T_\infty}, \quad \phi(\eta) = \frac{C - C_\infty}{C_w - C_\infty}, \quad (10)$$

Where η is the similarity variable and ψ is the stream function. $u = \partial\psi / \partial y$ and $v = -\partial\psi / \partial x$ are the velocity components, which identically satisfies Eq. (1).

Now substituting Eqs. (9) and (10) into the Eqs. (2)-(4), we get

$$f''' + ff'' - (f')^2 - A\left(f' + \frac{1}{2}\eta f''\right) + Gr\theta + Gc\phi - M \sin^2(\xi) f' - \frac{1}{K_3} f' = 0 \quad (11)$$

$$\frac{(1+R)}{Pr} \theta'' + f\theta' - f'\theta - A\left(\theta + \frac{1}{2}\eta\theta'\right) + \frac{(A^* f' + B^* \theta)}{Pr} + Ec(f'')^2 = 0 \quad (12)$$

$$\frac{1}{Sc} \phi'' + f\phi' - f'\phi - A\left(\phi + \frac{1}{2}\eta\phi'\right) - \gamma\phi = 0 \quad (13)$$

where $A = \frac{c}{a}$ is the unsteadiness parameter, $Gr = \frac{g\beta x(T_w - T_\infty)}{U_w^2}$ is the Grashof number,

$Gc = \frac{g\beta^* x(c_w - c_\infty)}{U_w^2}$ is the solutal Grashof number, $M = B_0^2 \left(\frac{\sigma}{\rho a}\right)$ is the Hartmann number,

$K_3 = \frac{ak_2}{\nu}$ is the permeability parameter, $R = \frac{16\sigma^* T_\infty^3}{3kk^*}$ is the radiation parameter, $Pr = \frac{\mu cp}{k}$ is the

Prandtl number, $Ec = \frac{U_w^2}{C_p(T_w - T_\infty)}$ is the Eckert number, $Sc = \frac{\nu}{D}$ is the Schmidt number and $\gamma = \frac{\Gamma_0}{a}$ is

the chemical reaction parameter.

The corresponding boundary conditions are

$$f = S, \quad f' = 1 + S_f f''(0), \quad \theta = 1 + S_t \theta'(0), \quad \phi = 1 + S_c \phi'(0) \quad \text{at } \eta = 0$$

$$f' \rightarrow 0, \quad \theta \rightarrow 0, \quad \phi \rightarrow 0 \quad \text{at } \eta \rightarrow \infty \quad (14)$$

In Eq. (14), S correspond to injection/suction parameter and $S_f = N_0 \rho \sqrt{av}$ is the nondimensional velocity slip, $S_t = K_0 \sqrt{a/\nu}$ is the thermal slip and $-S_c = P_0 \sqrt{a/\nu}$ is the solutal slip. In this study, the quantities of practical interest are skin friction coefficient, heat transfer rate and mass transfer which are defined as

$$C_f = \frac{\tau_w}{\rho U_w^2 / 2}, \quad Nu_x = \frac{xq_w}{k(T_w - T_\infty)}, \quad Sh_x = \frac{m_w x}{\rho D(c_w - c_\infty)} \quad (15)$$

$$\text{Where } \tau_w = \mu \left(\frac{\partial u}{\partial y} \right)_{y=0}, \quad q_w = -k \left(\frac{\partial T}{\partial y} \right)_{y=0}, \quad m_w = -\rho D \left(\frac{\partial c}{\partial y} \right)_{y=0} \quad (16)$$

Dimensionless skin friction coefficient, Nusselt number and the Sherwood number are expressed as:

$$C_f = \frac{1}{2} \text{Re}_x^{-\frac{1}{2}} f''(0), \quad Nu_x = -\text{Re}_x^{-\frac{1}{2}} \theta'(0), \quad Sh_x = -\text{Re}_x^{-\frac{1}{2}} \phi'(0) \quad (17)$$

3. Numerical estimates and related discussion

The dimensionless velocity, temperature and concentration distributions are obtained by using the fourth order Runge-Kutta method with shooting technique. Figure 1 displays that the velocity of the fluid reduces with large values of M for steady and unsteady flows, due to the application of Lorentz force. The influence of permeability parameter on velocity profile can be seen in Figure 2. The dimensionless linear momentum of the fluid increases with an intensification of permeability for steady and unsteady flows. For high permeability ($K_3 = 0.3; 0.5$), the axial velocity rises quicker than the case when the permeability is lower ($K_3 = 0.1$). Further one can note that the same pattern of velocity profiles is observed for steady and unsteady cases. The velocity profile for various values of aligned angle ζ as shown in Figure 3. The velocity profile of the fluid decreases with increasing the aligned angle for both steady and unsteady cases. Figure 4 depicts profile of temperature versus thermal radiation parameter. The thermal boundary layer of the fluid reduces with high values of thermal radiation parameter.

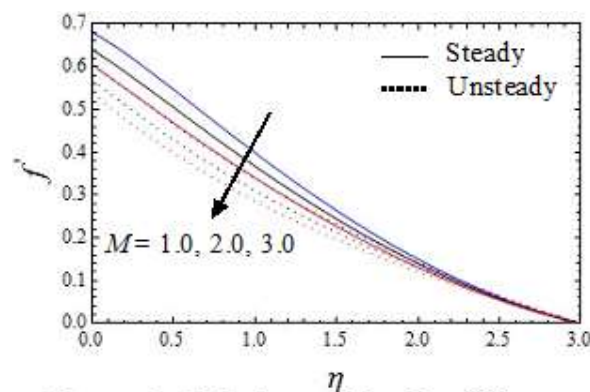


Figure 1. Velocity profiles for different values of M

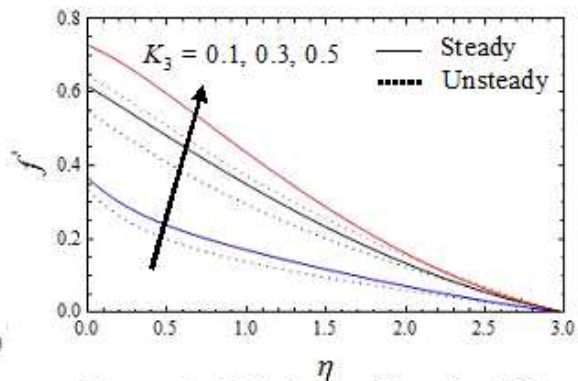


Figure 2. Velocity profiles for different values of K_3

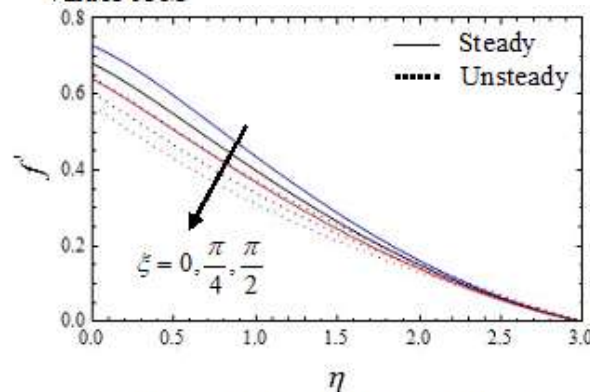


Figure 3. Velocity profiles for different values of ζ

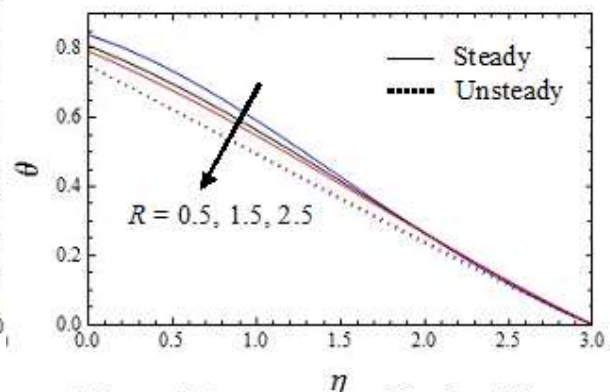


Figure 4. Temperature profiles for different values of R

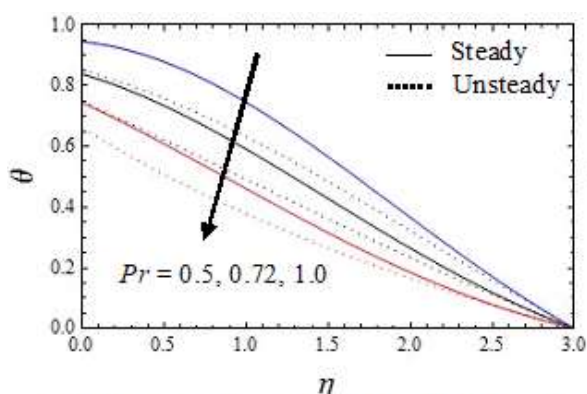


Figure 5. Temperature profiles for different values of Pr

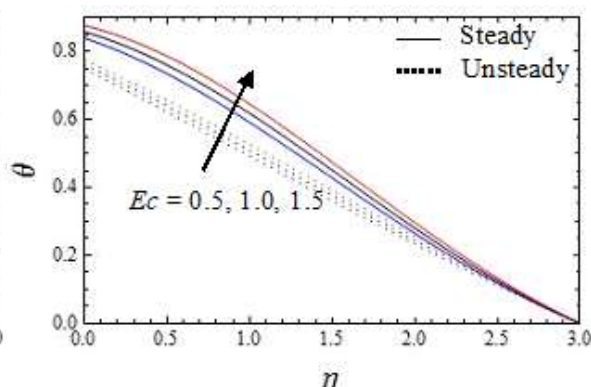


Figure 6. Temperature profiles for different values of Ec

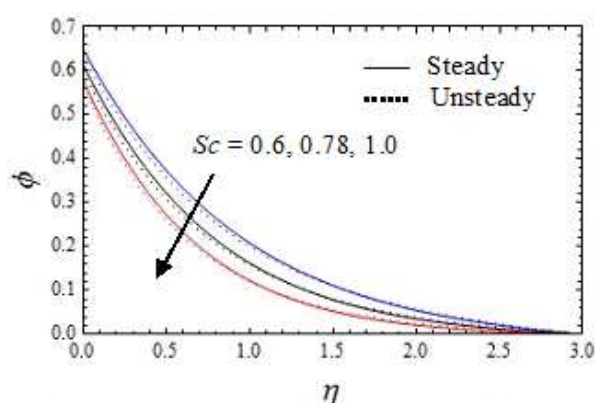


Figure 7. Concentration profiles for different values of γ

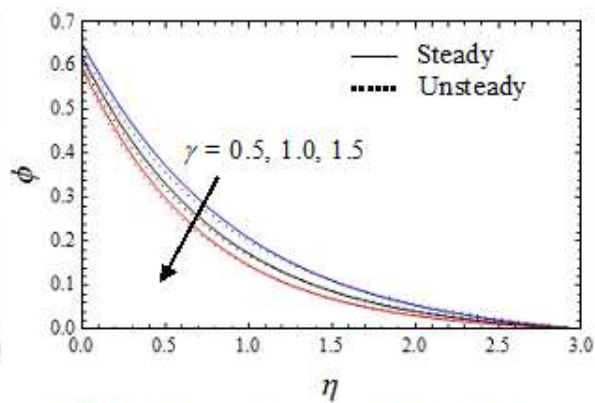


Figure 8. Concentration profiles for different values of Sc

Figure 5 shows the effect of Prandtl number (Pr) on the temperature. The thermal boundary layer thickness reduces for large values of Pr . Due to the cause of low values of Pr are equivalent to increasing the thermal conductivity of the fluid. The effect of Ec , on temperature is shown in Figure 6. As Ec is enhanced the temperature increases, since internal energy is increased. It is also seen from this figure that the temperature is less for the unsteady case when compared with steady case near the surface and then the temperature descends smoothly towards zero. Figure 7 shows the concentration distribution for Sc . In this figure, we noticed that the concentration of the fluid reduces at higher values of Sc . Figure 8 shows the variation of the γ on the concentration profiles. It reveals that the higher values of γ , the concentration profile decreases.

Table 1. Comparison table showing the computations $f''(0)$ for various values of A when $M = K_3 = Gr = Gc = Sc = A^* = B^* = S_f = S_t = S_c = 0$.

A	Pal et al. [16]	Srinivas et al. [17]	Present
0.8	-1.26104	-1.26108	-1.26108
1.2	-1.37772	-1.37777	-1.37777
2.0	-1.58736	-1.58741	-1.58741

Table 2. computations showing data of $-f''(0)$, $-\theta'(0)$ and $-\phi'(0)$ when $S_f=1.5$, $S_t=1.0$, and $S_c=0.5$ for both cases $A=0$ and $A=0.5$.

M	Gr	Gc	ξ	A^*	B^*	γ	$A=0$			$A=0.5$		
							$-f''(0)$	$-\theta'(0)$	$-\phi'(0)$	$-f''(0)$	$-\theta'(0)$	$-\phi'(0)$
1.0	2.0	2.0	$\pi/4$	0.5	0.5	0.5	0.212867	0.161136	0.700642	0.264000	0.251033	0.729856
2.0	2.0	2.0	$\pi/4$	0.5	0.5	0.5	0.239919	0.156875	0.691808	0.287270	0.249833	0.723126
1.0	3.0	2.0	$\pi/4$	0.5	0.5	0.5	0.642143	1.17700	0.289564	0.199729	0.253959	0.748295
1.0	2.0	3.0	$\pi/4$	0.5	0.5	0.5	0.170064	0.165366	0.71266	0.222787	0.252104	0.740304
1.0	2.0	2.0	$\pi/2$	0.5	0.5	0.5	0.239919	0.156875	0.691808	0.287270	0.249833	0.723126
1.0	2.0	2.0	$\pi/4$	1.0	0.5	0.5	0.618869	1.35066	0.397211	0.232326	0.125914	0.740281
1.0	2.0	2.0	$\pi/4$	0.5	1.5	0.5	0.454887	0.893873	0.568339	0.505811	1.008930	0.616328
1.0	1.0	2.0	$\pi/4$	0.5	0.5	1.0	0.220975	0.159539	0.75916	0.220975	0.159539	0.759160

Table 3. computations showing data of $-f''(0)$, $-\theta'(0)$ and $-\phi'(0)$ when $M=1.0$, $K_3=0.4$, $Gr=2.0$, $Gc=2.0$, $\xi = \pi/4$, $R=0.5$, $Pr=0.72$, A^* , B^* , $Ec=0.5$, $Sc=0.6$, and $\gamma = 0.5$ for $A=0$, and $A=0.5$,

S_f	S_t	S_c	$A=0$			$A=0.5$		
			$-f''(0)$	$-\theta'(0)$	$-\phi'(0)$	$-f''(0)$	$-\theta'(0)$	$-\phi'(0)$
0.5	0.5	0.5	0.428400	0.193419	0.711930	0.527545	0.305941	0.743065
1.0	0.5	0.5	0.274811	0.195771	0.706551	0.338107	0.310468	0.737009
0.5	1.0	0.5	0.449596	0.157793	0.709203	0.557709	0.244537	0.739663
0.5	0.5	1.0	0.47589	0.189120	0.522077	0.573978	0.303252	0.539268

In Table 1, we compared the present result corresponding to the $f''(0)$ having the excellent results. computations showing data of $-f''(0)$, $-\theta'(0)$ and $-\phi'(0)$ when $S_f=1.5$, $S_t=1.0$, and $S_c=0.5$ for both cases $A=0$ and $A=0.5$ are shown in Table 2. It can be noted that the $-f''(0)$ increased with large value of solutal Grashof number whereas the opposite behaviour is observed in the case of a magnetic parameter, aligned angle and temperature dependent heat source for both cases $A=0$ and $A=0.5$. The $-\theta'(0)$ increases with an increase in the Grashof number, solutal Grashof number, and temperature dependent heat source, where as it decreases with an high values of the magnetic parameter, aligned angle and chemical reaction parameter for both cases. It is observed that the $-\phi'(0)$ decreases as magnetic parameter, aligned angle and temperature dependent heat source increases for $A=0$ and $A=0.5$. The $-\phi'(0)$ increases with increasing solutal Grashof number and chemical reaction parameter for both cases. The surface skin friction, heat transfer rate and mass transfer rate for S_f , S_t and S_c at $A=0$ and $A=0.5$ are shown in Table 3. The $-f''(0)$ decreases with S_t and S_c , while it increases with the S_f for $A=0$ and $A=0.5$. The $-\theta'(0)$ decreases with the S_t and S_c while a slight increment is seen for enhancement of S_f for both cases. The value of $-\phi'(0)$ decreases with high values of S_f , S_t and S_c for $A=0$ and $A=0.5$.

4. Conclusion

This paper presents the study of the unsteady hydromagnetic heat and mass transfer of a Newtonian fluid in a permeable stretching surface with viscous dissipation. The effect of chemical reaction on the blood has more attracted by the investigators because the numerical calculation of blood flow rate is

the more important for identifying the nature (cause of some phenomenon) of blood circulation illness. The velocity profile increases with permeability parameter K_3 and decreases with Hartmann number M , and aligned angle ξ . The temperature of the fluid is low for high radiation parameter R and Prandtl number Pr and increases with Eckert number Ec . The concentration profile decreases with increasing the chemical reaction parameter γ . Aligned angle strengthens the magnetic field parameter and it has the capability to reduce the skin-friction. The value of skin-friction number decreases with increasing S_f , S_i and S_c .

References

- [1] Mastroberardino A 2014 *Applied Mathematics and Mechanics* **35**, 133-142.
- [2] Byron Bird R Warren E Stewart and Edwin Lightfoot N 1960 *Transport phenomena*, (John Wiley and sons, New York).
- [3] Bala Anki Reddy P 2016 *Journal of Naval Architecture and Marine Eng.* **13** 165-177.
- [4] Themelis N J 1995 *Taylor & Francis Group*.
- [5] P. Bala Anki Reddy P 2016 *Ain Shams Eng. J.* **7** 593-602.
- [6] Midya C, *Chinese Physics Letters* **29** 014701.
- [7] Srinivas S, Reddy P B A and Prasad B S R V 2015 *Heat transfer-Asian Research* **44** 172-187.
- [8] Suneetha S and Bala Anki Reddy P 2016 *RJPT* **9(12)** 2-7.
- [9] Yan Zhang, Min Zhang, and Shujuan Qi 2016 *Mathematical Problems in Engineering* **2016** 8521580.
- [10] Sharidan S Mahmood T and Pop I 2006 *Int. J. Appl. Mech. Eng.* **11** 647-654.
- [11] Bala Anki Reddy P and Vijaya Sekhar D, *International journal of Engineering Research and Applications* **3** 572-581.
- [12] Pal D 2011 *Commun. Nonlinear Sci. Numer. Simulat.* **16** 1890-1904
- [13] Srinivas S, Reddy P B A and Prasad B S R V 2014 *J. mech. med. biol.* **14** 1450067.
- [14] Jena S Dash G C and Mishra S R 2016 *Ain Shams Eng. J.*
- [15] Bala Anki Reddy P and Bhaskar Reddy N 2011 *Int. J. Appl. Math. Comput.* **3** 300-306.
- [16] Brinkman H C 1951 *Appl. Sci. Res* **A2** 120-124.
- [17] G. Chand G and R.N. Jat R N 2014 *Therm. Energy Power Engg.* **3** 266-272.
- [18] Chamka A J Aly A M and Mansour M A 2010 *Chem. Eng. Comm.* **197** 846-858.